Cumhuriyet Science Journal

e-ISSN: 2587-246X
ISSN: 2587-2680

Cumhuriyet Sci. J., 42(4) (2021) 852-861
http://dx.doi.org/10.17776/csj.957198

Investigation of the catalytic effect of metal-metal oxide structure in the catalysts used in hydrogen production by electrolysis of water

Özkan AYDIN [1,*]

[1]*Osmaniye Korkut Ata University, Faculty of Engineering, Department of Chemical Engineering, Osmaniye / TURKEY*

Abstract

Hydrogen, which is obtained by water splitting using the electrolysis method, is one of the cleanest and most environmentally friendly energy carriers. However, since this production method is expensive, it is not preferred in industrial hydrogen production. Researchers working on this subject have intensified their studies to reduce costs. One of the most important factors determining the cost is the development of effective and inexpensive cathode and anode materials. In this study, the catalysts obtained by electrochemical deposition of nickel on the graphite rod, cobalt oxide using the drag effect and electrochemical platinum deposition on it, were used as the cathode material. The surface characterizations of the obtained catalysts were carried out using SEM and XRD techniques. The electrochemical properties of the catalysts were analyzed using electrochemical impedance spectroscopy, linear sweep voltammetry and potentiodynamic polarization methods. It was determined that the most effective nickel deposition time is 10 seconds, CoO content is 1.9 mg and platinum deposition time is 45 seconds. The initial potential for the hydrogen evolution reaction of the catalyst which has the highest catalytic efficiency was 75 mV and current density was determined as 500 mA cm^{-2} at the cathodic 0.5 V_{SHE} overvoltage.

Article info

History:
Received:24.06.2021
Accepted:02.11.2021

Keywords:
Hydrogen evolution,
Electrocatalyst,
Electrochemical analysis,
Electrochemical deposition,
Drag effect.

1. Introduction

In the world, the effects of global warming caused by greenhouse gases in the atmosphere caused by fossil fuels used to meet the world's increasing energy needs are being felt day by day. [1, 2]. Therefore, the demand for clean and renewable energy sources is increasing day by day. [3]. Hydrogen is preferred as an alternative clean energy source to fossil fuels due to its high energy density, abundance, and environmental friendliness. [4, 5]. There are many methods for producing hydrogen. About 50% of global hydrogen demand is met by natural gas steam reform, 30% by oil reform, 18% by coal gasification, 3.9% by electrolysis of water and 0.1% by other sources [6-9]. To eliminate the negative effects of fossil fuel use on the environment, human health and climate, it is necessary to produce hydrogen from clean and abundant sources with environmentally friendly methods. [10-14]. The name of this hydrogen production method is green hydrogen production. Hydrogen production by electrolysis of water is one of the green production technologies. The purity of the hydrogen obtained by this method is quite high. However, one of the main problems of this production method is that the production cost is high compared to other methods. Developing effective and inexpensive cathode and anode materials in electrolysis processes has an important place in terms of cost. Therefore, researchers focused on the development of catalysts for a low-cost effective anode and cathode material. [15]. Different combinations of catalysts are formed using a single metal[16-18], binary [19-24], ternary metal alloys [25-27] or metal oxides[28-31]. These combinations can be obtained by attaching to the support electrode with different applications such as metallurgical sintering method [24], electrochemical deposition method [32-34], slurry application method [35] or spray coating method [31, 36]. In these applications, nickel-based catalysts are one of the most widely used metals because they are electrochemically advantageous and relatively inexpensive. [37-41]. Another element that is frequently used in the reactions of obtaining hydrogen by the electrolysis of water is cobalt and its oxide compounds. [31, 42-44] . Noble metals are often added in trace amounts to reduce the hydrogen evolution overvoltage. [45]. Platinum is one of the

*Corresponding author. *e-mail address: ozkanaydin@osmaniye.edu.tr*

noble metals most capable of producing hydrogen among these noble metals.

In this study, metallic nickel (Ni) was electrochemically deposited on a graphite rod (C). It is known that metal oxides create a synergistic effect with metals. [30]. Therefore, during metallic nickel deposition, nano-structured cobalt oxide (CoO) was added to the nickel deposition bath and suspended in the solution to attach the surface by the drag effect. Finally, trace amounts of platinum (Pt) were electrochemically deposited on the Ni-CoO combination. The obtained catalysts were electrochemically analyzed for hydrogen evolution reaction in alkaline medium using electrochemical impedance spectroscopy (EIS), linear sweep voltammetry (LSV), and potentiodynamic polarization techniques.

2. Experimental Method

2.1. Material and method

Cylindrical graphite rods of 10 cm length were used as support electrodes in the experiments. These rods are insulated with polyester material, leaving only the lower ends open. The area of this active circular part that remains open is 0.283 cm^2. Before each experiment, these rods were sanded with 1200 grit sandpaper, then washed with distilled water, acetone and again with distilled water, respectively. The cobalt oxide nanoparticles used in the study were synthesized as follows; 50 ml 0.6 M $Co(NO_3)_2$. $6H_2O$ (Fluka, ≥ 98%) at 50℃ which was filled into a burette was added to 50 ml 3.2 M NaOH (Sigma-Aldrich, ≥ 99%) at 50℃ which is mixed dropwise. Then, 50 ml H_2O_2 (Merck , 50 % w/w) was added dropwise by using burette to this stirred solution. The precipitate was filtered off and washed with distilled water. The resulting precipitate was dried at 110℃ for 10 hours [46]. Electrochemical deposition and analyzes were performed using potentiostat (Gamry interface 1000E).

Three electrode techniques were used for electrochemical analyzes. Here, Pt sheet with a surface area of 2 cm^2 as the anode (CE), Ag / AgCl as the reference electrode, and catalysts loaded on the graphite rod as the cathode (WE) were used. In these analyses, 1.0 M KOH solution was used as the electrolyte. EIS, LSV and potentiodynamic polarization techniques were used to determine the catalytic efficiency for hydrogen production. EIS measurements were obtained in the frequency range of 10^6 to 0.01 Hz with an amplitude of 10 mV. LSV measurements were made at a scan rate of 1 mV s^{-1} between 0 V and cathodic 0.5 V.

2.2. Experimental

Graphite rods were electrochemically coated with a current density of 340.0 mA cm^{-2} in a nickel bath, the composition of which is given in Table 1. Therefore, three different deposition times (10, 60, and 110 s) were applied and denoted as **Ni_t.** Here t represents the nickel deposition time.

Table 1. Compositions of electrochemical deposition baths for Ni and Pt.

	$NiSO_4$.$6H_2O$	H_3BO_3	$NiCl_2.6H_2O$	K_2PtCl_6	Total Volume
Ni Bath	30 g	1.25 g	1 g	---	100 mL
Pt Bath	---	---	---	0,1M (pH=1)	100 mL

After determining the most effective deposition time for nickel, CoO nanoparticles were added into the nickel bath and suspended solution was obtained. In this way, while nickel deposition is done electrochemically, CoO is also deposited on the surface with the drag effect. In this section, five different CoO amounts (0.1 mg, 1.0 mg, 1.3 mg, 1.9 mg, and 3.7 mg CoO) were prepared and the obtained catalysts were denoted as Ni_t-$CoO_{(Xmg)}$. Here x represents the amount of CoO added to the nickel-plating bath. Finally, platinum (Pt) was electrochemically deposited on Ni_t-$CoO_{(Xmg)}$ catalyst. In this section, metallic platinum was deposited with a current density of 3,53 mA cm^{-2} in three different deposition times (15, 30, and 45 s). This obtained catalyst was denoted as Ni_t-$CoO_{(Xmg)}$_Pt_t.

After the Ni_t, Ni_t-$CoO_{(Xmg)}$, and Ni_t-$CoO_{(Xmg)}$_Pt_t catalysts were prepared, the efficiency of the obtained catalysts in terms of hydrogen production was analyzed using EIS, LSV and potentiodynamic polarization techniques. Total hydrogen production for the best catalysts was calculated using a reverse burette[28]. Hydrogen produced at the cathode was collected in the reverse burette and after one hour the

total volume of hydrogen produced was measured. Experiments were carried out at 20 ℃ and under 736 mmHg pressure. Pt electrode was used as the anode and 1.0 M KOH solution was used as the electrolyte. Surface characterization and elemental analyses of the catalysts were carried out with Field emission scanning electron microscope (FEI Quanta 650 Field Emission SEM) coupled with energy dispersive X-ray (EDX). The powder XRD measurements were performed with PANalytical EMPYREAN, 2θ angle between 5° and 90°.

3. Results and Discussion

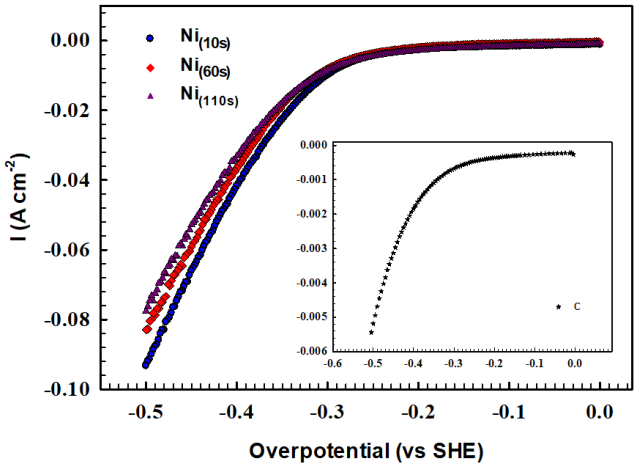

Figure 1. LSV diagrams of C, $Ni_{(10s)}$, $Ni_{(60s)}$, and $Ni_{(110s)}$ catalyst.

EIS measurements at the overvoltage region provide information about the charge transfer resistance of catalyst for hydrogen evolution reaction. The Nyquist graphs obtained for the prepared catalysts at -0.3 V_{SHE} in 1.0 M KOH solution were given in Fig. 2. The Nyquist graph for C is given in the inset graph. When Fig. 2 is examined, it is seen that all catalysts have a time constant due to charge transfer resistance and $Ni_{(10s)}$ catalyst has the lowest charge transfer resistance.

It is known that metal-metal oxide composition has positive effects for catalysts used in hydrogen production [28]. Therefore, the effect of CoO on the HER was investigated by adding to the catalyst structure. Metal oxides are usually attached to the catalyst structure using conductive adhesives such as Polyvinylidene fluoride and carboxymethyl cellulose. These adhesives create additional resistance. To avoid such negative effects, CoO nanoparticles were added to the catalyst structure by the drag effect during electrochemical nickel deposition. Different amounts of CoO (0.1 mg, 1 mg, 1.3 mg, 1.9 mg, and 3.7 mg CoO) were added to the nickel deposition bath to obtain a suspended CoO nickel bath.

The LSV technique was used to characterize all the catalysts obtained for hydrogen evolution reaction (HER). The overvoltage-current density curves for different nickel-deposition times on the graphite rod (C) given in Fig. 1 were taken at a scan rate of 1 mV s^{-1} and in the range of 0 V and cathodic 0.5 V_{SHE}. When Fig. 1 is examined, the initial potential of the HER for C is -0.35 V. Initial potentials of HER for $Ni_{(10s)}$, $Ni_{(60s)}$ ve $Ni_{(110s)}$ were shown in Fig. 1 as -0.26 V, -0.30 V and -0.29 V, respectively.

Comparing the curves, it is seen that the highest cathodic current density and the lowest overvoltage for HER belong to $Ni_{(10s)}$ catalyst.

The effect of CoO attachment during nickel deposition was investigated for HER using LSV and EIS techniques. The overvoltage (vs. SHE) – current density plots of catalysts defined as Ni_t-$CoO_{(Xmg)}$ was given Fig. 3. When the figure is examined, the initial potentials of hydrogen evolution for $Ni_{(10s)}$, $Ni_{(10s)}$-$CoO_{(0.1mg)}$, $Ni_{(10s)}$-$CoO_{(1.0mg)}$, $Ni_{(10s)}$-$CoO_{(1.3mg)}$, $Ni_{(10s)}$-$CoO_{(1.9mg)}$ ve $Ni_{(10s)}$-$CoO_{(3.7mg)}$ catalysts were obtained as -0.26 V, -0.32 V, -0.34 V, -0.28 V, -0.22 V, and -0.27 V, respectively. Comparing the curves obtained for the prepared catalysts at -0.3 V_{SHE} overvoltage, it was determined that the highest current density was 19.6 mA cm^{-2} and the lowest overvoltage for HER was -0.22 V. These values belong to $Ni_{(10s)}$-$CoO_{(1.9mg)}$ catalyst.

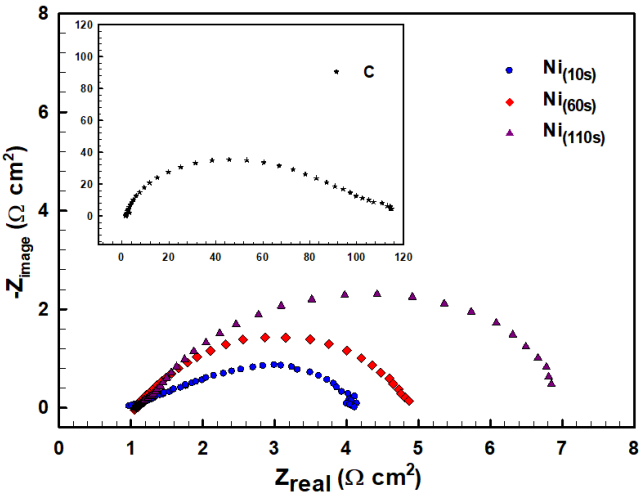

Figure 2. Nyquist diagrams of C, $Ni_{(10s)}$, $Ni_{(60s)}$ ve $Ni_{(110s)}$ catalyst

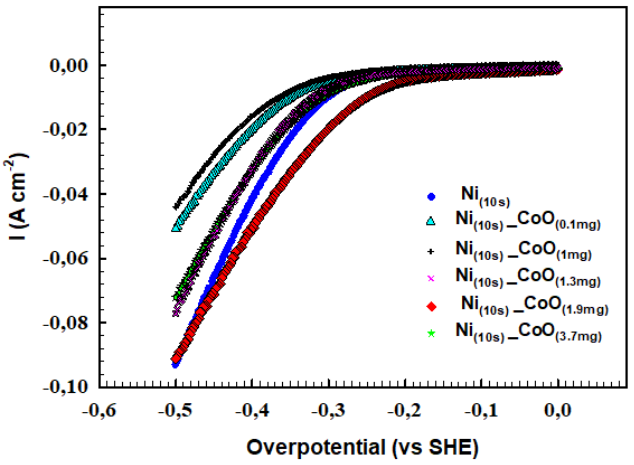

Figure 3. LSV diagrams of $Ni_{(10s)}$, $Ni_{(10s)}$-$CoO_{(0.1mg)}$, $Ni_{(10s)}$-$CoO_{(1.0mg)}$, $Ni_{(10s)}$-$CoO_{(1.3mg)}$, $Ni_{(10s)}$-$CoO_{(1.9mg)}$ and $Ni_{(10s)}$-$CoO_{(3.7mg)}$ catalysts

EIS measurements for $Ni_{(10s)}$, $Ni_{(10s)}$-$CoO_{(0.1mg)}$, $Ni_{(10s)}$-$CoO_{(1.0mg)}$, $Ni_{(10s)}$-$CoO_{(1.3mg)}$, $Ni_{(10s)}$-$CoO_{(1.9mg)}$ and $Ni_{(10s)}$-$CoO_{(3.7mg)}$ catalysts were taken in 1.0 M KOH solution and -0.3 V_{SHE} overvoltage were given in Fig. 4. When the curves in Fig. 4 were compared, it is seen that the lowest charge transfer resistance (2.6 Ω cm^2) belongs to $Ni_{(10s)}$-$CoO_{(1.9mg)}$ catalyst.

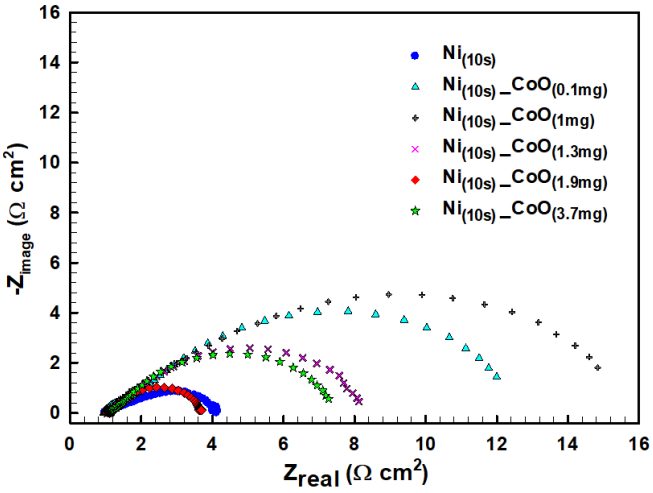

Figure 4. Nyquist diagrams of $Ni_{(10s)}$, $Ni_{(10s)}$-$CoO_{(0.1mg)}$, $Ni_{(10s)}$-$CoO_{(1.0mg)}$, $Ni_{(10s)}$-$CoO_{(1.3mg)}$, $Ni_{(10s)}$-$CoO_{(1.9mg)}$ and $Ni_{(10s)}$-$CoO_{(3.7mg)}$ catalysts

One of the noble metals, Pt, was electrochemically deposited on the $Ni_{(10s)}$-$CoO_{(1.9mg)}$ catalyst to increase the catalytic efficiency. Since it is a metal with high catalytic efficiency but expensive, so deposition times are kept short. Metallic Pt was deposited at a current density of 3.53 mA cm^{-2} in three different deposition times (15, 30 and 45 s). Prepared Ni_t-$CoO_{(Xmg)}$_Pt_t catalysts were electrochemically analyzed for HER activity using LSV and EIS techniques. Fig. 5 shows the overvoltage (vs. SHE) – current density plots of catalysts identified as Ni_t-$CoO_{(Xmg)}$_Pt_t. When the figure is examined, the starting potentials of hydrogen evolution of catalysts $Ni_{(10s)}$-$CoO_{(01.9mg)}$, $Ni_{(10s)}$-$CoO_{(1.9mg)}$_Pt_{15}, $Ni_{(10s)}$-$CoO_{(1.9mg)}$_Pt_{30}, and $Ni_{(10s)}$-$CoO_{(1.9mg)}$_Pt_{45} are seen as -0.22 V, -0.13 V, -0.10 V and -0.075 V, respectively. When the curves at -0.3 V_{SHE} overvoltage were compared for the prepared catalysts, the highest cathodic current density was found to be 80.0 mA cm^{-2} and the lowest overvoltage value for HER was - 75 mV. These values belong to $Ni_{(10s)}$-$CoO_{(1.9mg)}$_Pt_{45} catalyst.

To determine the catalytic activities of the platinum deposited catalysts, EIS measurements were taken at -0.3 V_{SHE} overvoltage. Nyquist plots for $Ni_{(10s)}$-$CoO_{(01.9mg)}$, $Ni_{(10s)}$-$CoO_{(1.9mg)}$_Pt_{15}, $Ni_{(10s)}$-$CoO_{(1.9mg)}$_Pt_{30}, and $Ni_{(10s)}$-$CoO_{(1.9mg)}$_Pt_{45} catalysts were given in Fig. 6. When the figure is examined, it is seen that the lowest charge transfer resistance belongs to $Ni_{(10s)}$-$CoO_{(1.9mg)}$_Pt_{45} catalyst and is 0.35 Ω cm^2.

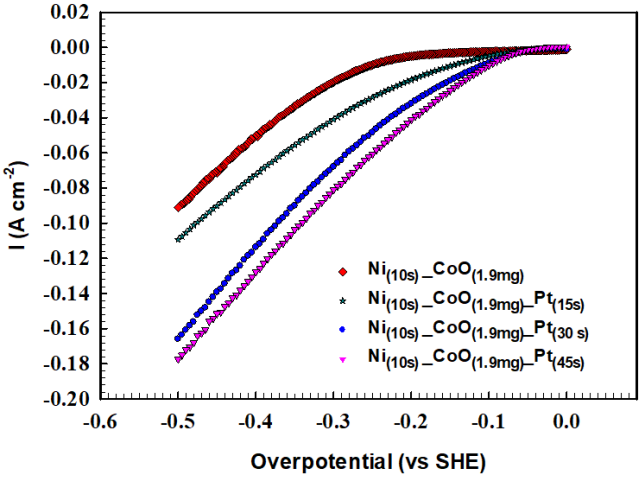

Figure 5. LSV diagrams of $Ni_{(10s)}$-$CoO_{(01.9mg)}$, $Ni_{(10s)}$-$CoO_{(1.9mg)}$_Pt_{15}, $Ni_{(10s)}$-$CoO_{(1.9mg)}$_Pt_{30}, and $Ni_{(10s)}$-$CoO_{(1.9mg)}$_Pt_{45} catalysts.

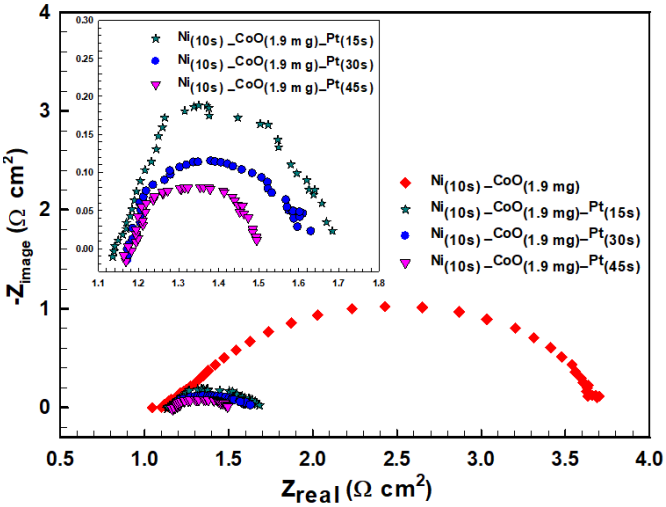

Figure 6. Nyquist diagrams of $Ni_{(10s)}$-$CoO_{(01.9mg)}$, $Ni_{(10s)}$-$CoO_{(1.9mg)}$_Pt_{15}, $Ni_{(10s)}$-$CoO_{(1.9mg)}$_Pt_{30}, and $Ni_{(10s)}$-

$CoO_{(1.9mg)}$_Pt_{45} catalysts. Comparisons of the LSV curves of $Ni_{(10s)}$-$CoO_{(1.9mg)}$_Pt_{45} catalyst and 20% (w/w) Pt/C catalysts purchased commercially from ERDES Technology ve Chemistry Company in terms of HER are given in Fig. 7.

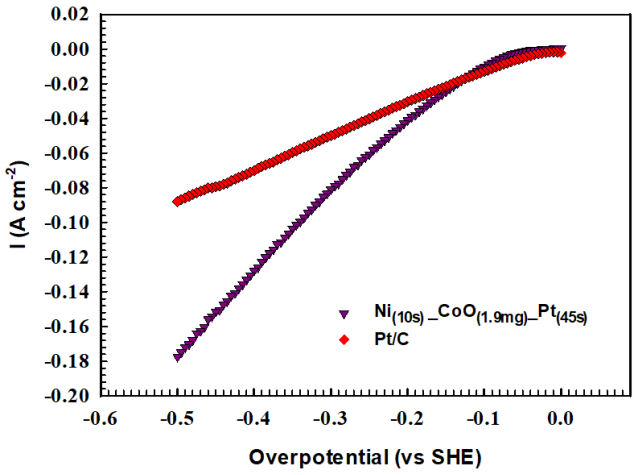

Figure 7. LSV diagrams of Pt/C and $Ni_{(10s)}$-$CoO_{(1.9mg)}$_Pt_{45} catalysts

Initial potentials for HER of commercial Pt/C catalyst and $Ni_{(10s)}$-$CoO_{(1.9mg)}$_Pt_{45} catalyst were measured as cathodic 28 mV and 75 mV, respectively. The Pt/C catalyst appears to be more efficient when comparing the initial potentials for hydrogen evolution. However, the current densities of Pt/C and $Ni_{(10s)}$-$CoO_{(1.9mg)}$_Pt_{45} catalyst at -0.5 V_{SHE} overvoltage were measured as 88 mA cm^{-2} and 500 mA cm^{-2}, respectively. This shows that the current density of $Ni_{(10s)}$-$CoO_{(1.9mg)}$_Pt_{45} catalyst at -0.5 V_{SHE} overvoltage is 5 times higher than the commercial catalyst.

The potentiodynamic polarization technique for catalysts $Ni_{(10s)}$, $Ni_{(10s)}$-$CoO_{(1.9mg)}$, and $Ni_{(10s)}$-$CoO_{(1.9mg)}$_Pt_{45} was applied at a scan rate of 10 mV s^{-1}, in 1.0 M KOH solution in the range of 0 to 300 mV. Obtained data are graphed in Fig. 8. Current densities at some overvoltages, 50, 100 and 200 mV were used to compare the catalytic efficiency. Current densities at given overvoltages, Tafel constant (b) and i_0 (-a/b), were given in Table 2.

Table 2. Electrochemical data obtained from cathodic potentiodynamic polarization curves at different potentials.

	$-\eta_{50}$ (mA cm^{-2})	$-\eta_{100}$ (mA cm^{-2})	$-\eta_{200}$ (mA cm^{-2})	i_0 (mA cm^{-2})	b (mV dec^{-1})
$Ni_{(10s)}$	2.87	2.80	2.58	3.11	288.71
$Ni_{(10s)}$-$CoO_{(1,9mg)}$	2.73	2.62	2.29	2.97	248.62
$Ni_{(10s)}$-$CoO_{(1,9mg)}$-$Pt_{(45s)}$	2.84	2.32	1.39	4.04	73.53

When the current densities obtained at a constant overvoltage are compared, it is seen that the $Ni_{(10s)}$-$CoO_{(1.9mg)}$_Pt_{45} catalyst has a higher catalytic activity than the others. When the Tafel constant (b) values given in Fig. 8 are compared, the b values of $Ni_{(10s)}$ and $Ni_{(10s)}$-$CoO_{(1.9mg)}$ catalysts have a value greater than 120, and the b value for $Ni_{(10s)}$-$CoO_{(1.9mg)}$_Pt_{45} catalyst is less than 120. It can be understood that the hydrogen adsorption mechanism for the three catalysts is controlled according to Volmer- Heyrovsky mechanism. It is also seen that the rate determining reaction step for catalysts $Ni_{(10s)}$ and $Ni_{(10s)}$-$CoO_{(1.9mg)}$ is Volmer and the rate determining reaction step for catalyst $Ni_{(10s)}$-$CoO_{(1.9mg)}$_Pt_{45} is Heyrovsky mechanism.

Hydrogen evolution experiments in 1.0 M KOH solution using Pt/C, C, $Ni_{(10s)}$, $Ni_{(10s)}$-$CoO_{(1.9mg)}$ ve $Ni_{(10s)}$-$CoO_{(1.9mg)}$_Pt_{45} catalysts were carried out for 1 hour and at a current density of 200 mA cm^{-2}.

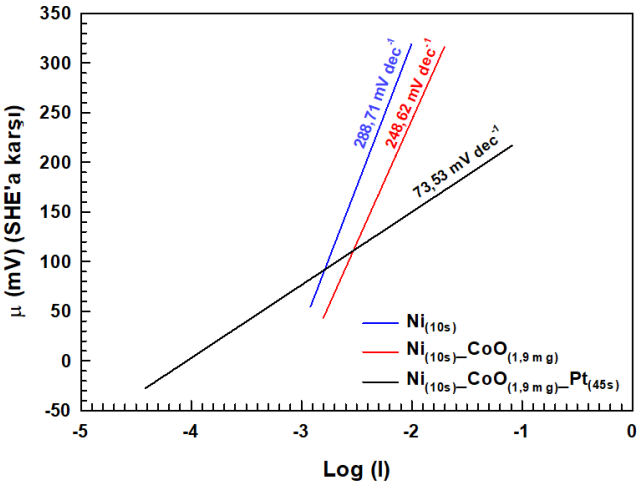

Figure 8. Cathodic potentiodynamic polarization curves of $Ni_{(10s)}$, $Ni_{(10s)}$-$CoO_{(1,9mg)}$, and $Ni_{(10s)}$-$CoO_{(1,9mg)}$_Pt_{45} catalysts obtained in 1.0 M KOH solution.

The results were given in Table 3. When the results are compared in terms of hydrogen production potential, it is seen that $Ni_{(10s)}$-$CoO_{(1.9mg)}$_Pt_{45} catalyst was more

effective. Considering the LSV curves in Fig. 7, it is seen that Pt/C is more effective at hydrogen output potential, but $Ni_{(10s)}$-$CoO_{(1.9mg)}$_Pt_{45} catalyst was more effective at higher overvoltages (≥ cathodic -150 mV). The hydrogen generation potentials in the overvoltage region in Table 3 confirm this.

Table 3. Hydrogen production amounts of catalysts.

	C	$Ni_{(10s)}$	$Ni_{(10s)}$-$CoO_{(1.9mg)}$	$Ni_{(10s)}$-$CoO_{(1.9mg)}$_Pt_{45}	Pt/C
Hydrogen Volume	82.8 mL cm^{-2}	85.4mL cm^{-2}	86.2 mL cm^{-2}	88.9 mL cm^{-2}	87.2 mL cm^{-2}

XRD measurements were made on the PANalytical EMPYREAN instrument. XRD measurements of $Ni_{(10s)}$-$CoO_{(1.9mg)}$_Pt_{45} catalyst were given in Fig. 9. The peaks in the figure were defined using JCPDF No. 98-005-3781 (C), JCPDF No. 98-026-0169 (Ni), andJCPDF No. 98-010-5069 (Pt) reference cards. When the XRD graph was examined, two peaks belonging to C at 26.2 and 77.2, one peak belonging to Ni at 53.6 and two peaks belonging to Pt at 42.5 and 82.8 were determined. The peak of CoO was not observed in the XRD graph. This is because CoO was attached to the structure by the drag effect during nickel deposition, so it remained under the nickel plate. Observation of the C peak in the structure supports that the surface was not completely covered and a catalyst with a porous structure was obtained.

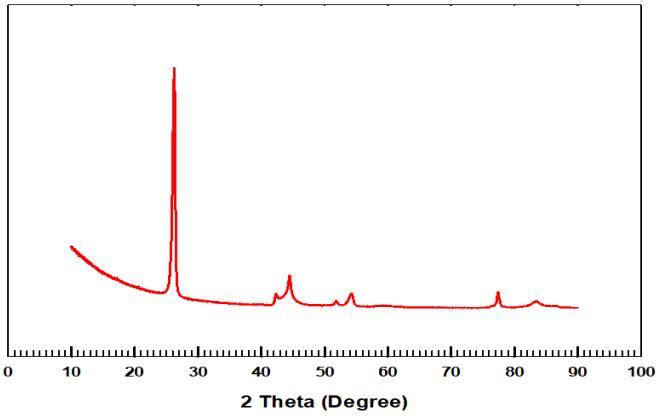

Figure 9. XRD pattern of $Ni_{(10s)}$-$CoO_{(1.9mg)}$_Pt_{45} catalyst.

SEM images of C (a), $Ni_{(10s)}$ (b), $Ni_{(10s)}$-$CoO_{(1.9mg)}$ (c) ve $Ni_{(10s)}$-$CoO_{(1.9mg)}$_Pt_{45} (d) catalysts taken with 10.0 kx magnification were given in Fig. 10. In Fig. 10a, carbon layers stacked on top of each other in the form of leaves are seen. Uniformly deposited nickel layers are shown in Fig. 10b. In Figure 10c, the presence of CoO in the structure is understood from the morphological differences in the structure due to the CoOs attached to the structure during nickel deposition. Finally, in Figure 10d, it is clearly seen that Pt is uniformly coated on the catalyst surface electrochemically, with a size of about 20-40 nm.

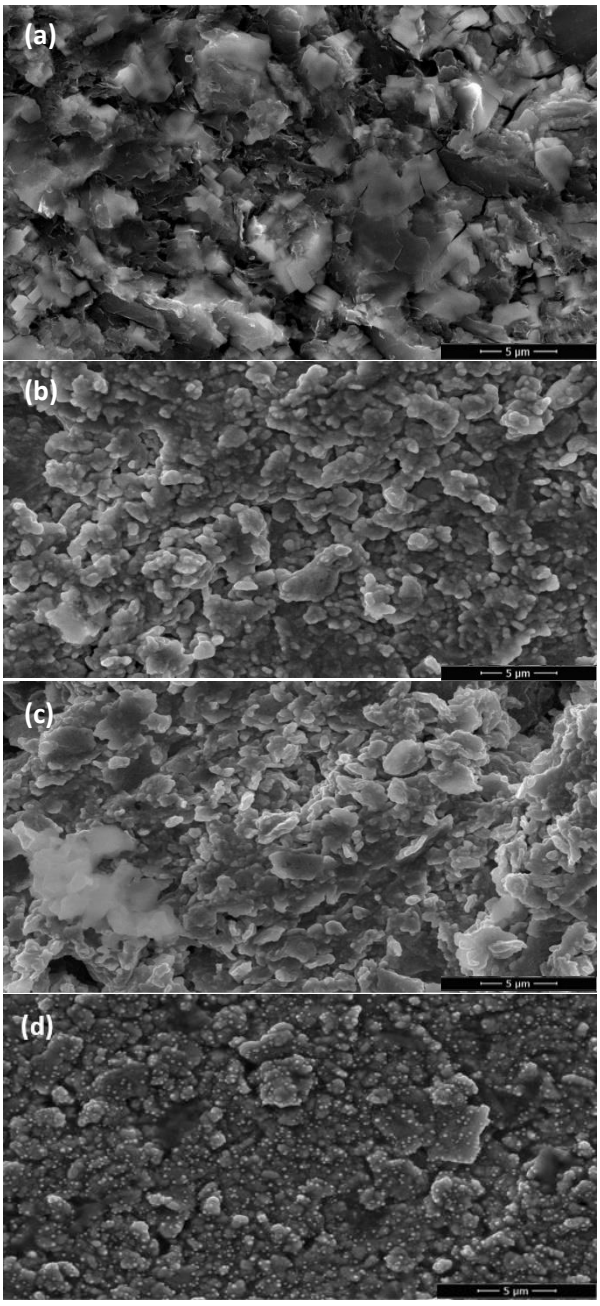

Figure 10. SEM images of C (a), Ni(10s) (b), Ni(10s)-CoO(1.9mg) (c), and Ni(10s)-CoO(1.9mg)_Pt45 (d) catalysts taken at 10.0 kx magnification.

In addition, the surface composition and surface homogenization characterization of $Ni_{(10s)}$-$CoO_{(1.9mg)}$_Pt_{45} catalyst using EDX and elemental mapping techniques were given in Fig. 11. When the figure is examined, it is seen that Nickel and CoO are uniformly deposited on the catalyst surface.

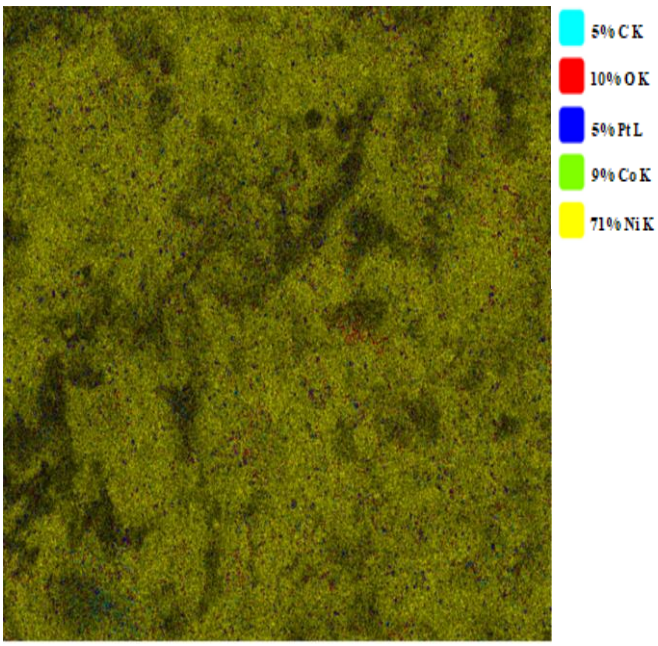

Figure 11. Mapping and EDX results of $Ni_{(10s)}$-$CoO_{(1,9mg)}$_Pt_{45} catalyst

Conclusions

In this study, catalysts with increased catalytic efficiency were obtained for HER by electrochemically deposited different compounds consisting of Ni, CoO and Pt on carbon support. All the obtained catalysts were analyzed by LSV and EIS techniques. In the nickel deposition process on carbon support, the most effective time for HER was determined as 10 seconds at 96 mA cm^{-2} and was shown as $Ni_{(10s)}$. CoO was added to the catalyst structure due to the catalytic efficiency-enhancing effect of metal-metal oxide structures for HER. In the process of adding CoO to the catalyst structure, the metal oxide was electrochemically deposited with a drag effect simultaneously during nickel deposition because avoid the negative effects of conductive adhesives. For deposition, different amounts of CoO were added to the Nickel bath and the most effective catalyst for HER was obtained when 1.9 mg of CoO was added, and it was symbolized as Ni(10s)-CoO(1.9mg). The catalytic activities of noble metals are known. To increase the catalytic efficiency, traces of noble metals (Pt) were added electrochemically to the catalyst structure. Because Pt is quite expensive compared to other metals. Therefore, different deposition times were applied and the Pt deposition time for the most effective catalyst was determined as 45 seconds and obtained catalyst was denoted as $Ni_{(10s)}$-$CoO_{(1.9mg)}$_Pt_{45}. Elemental and surface characterizations of the obtained catalysts were made using SEM-EDX and XRD devices. According to these analyzes, it was observed that Ni, CoO and Pt were homogeneously distributed on the surface. The hydrogen production capabilities of the obtained catalysts were tested with the reverse burette method and it was determined that the $Ni_{(10s)}$-$CoO_{(1.9mg)}$_Pt_{45} catalyst was more effective than the others. According to the potentiodynamic polarization technique, the hydrogen adsorption mechanism for the three catalysts is controlled by Volmer- Heyrovsky mechanism. It is also seen that the rate-determining reaction step for catalysts Ni(10s) and Ni(10s)-CoO(1.9mg) is Volmer and the rate-determining reaction step for catalyst $Ni_{(10s)}$-$CoO_{(1.9mg)}$_Pt_{45} is Heyrovsky mechanism.

Acknowledgment

The author would like to especially thanks Osmaniye Korkut Ata University for the scientific project department (OKÜBAP-2020-PT2-004), OKUMERLAB, and Assoc. Prof. Dr. Murat FARSAK.

Conflicts of interest

Related to the paper “Investigation of the Catalytic Effect of Metal-Metal Oxide Structure in the Catalysts Used in Hydrogen Production by Electrolysis of Water” submitted to the Cumhuriyet Science Journal, I declare that there is no financial/personal interest or belief that could affect our objectivity, and that no potential conflict exists.

References

[1] Höök M., Tang X., Depletion of fossil fuels and anthropogenic climate change—A review, *Energ Policy*, 52(1) (2013) 797-809.

[2] Luo M., Yi Y., Wang S., Wang Z., Du M., Pan J., Wang Q., Review of hydrogen production using chemical-looping technology, *Renewable and Sustainable Energy Reviews*, 81(2) (2018) 3186-214.

[3] Wang Y., Yang X., Wang Y., Catalytic performance of mesoporous MgO supported Ni catalyst in steam reforming of model compounds of biomass fermentation for hydrogen production, *International Journal*

of Hydrogen Energy, 41(40) (2016) 17846-57.

[4] Gong M., Wang D-Y., Chen C-C., Hwang B-J., Dai H., A mini review on nickel-based electrocatalysts for alkaline hydrogen evolution reaction, *Nano Research*, 9(1) (2016) 28-46.

[5] Zhang F., Zhao P., Niu M., Maddy J., The survey of key technologies in hydrogen energy storage, *International Journal of Hydrogen Energy*, 41(33) (2016) 14535-14552.

[6] Dincer I., Acar C., Review and evaluation of hydrogen production methods for better sustainability, *International Journal of Hydrogen Energy*, 40(34) (2015) 11094-11111.

[7] Muradov N., Veziroğlu T., From hydrocarbon to hydrogen–carbon to hydrogen economy, *International journal of hydrogen energy*, 30(3) (2005) 225-237.

[8] Arregi A., Amutio M., Lopez G., Bilbao J., Olazar M., Evaluation of thermochemical routes for hydrogen production from biomass: A review, *Energy Conversion and Management*, 165(1) (2018) 696-719.

[9] Holladay JD., Hu J., King DL., Wang Y., An overview of hydrogen production technologies, *Catalysis Today*, 139(4) (2009) 244-60.

[10] Levin DB., Chahine R., Challenges for renewable hydrogen production from biomass, *International Journal of Hydrogen Energy*, 35(10) (2010) 4962-4969.

[11] Bowen CT., Davis HJ., Henshaw BF., Lachance R., LeRoy RL., Renaud R., Developments in advanced alkaline water electrolysis, *International Journal of Hydrogen Energy*, 9(1) (1984) 59-66.

[12] Pu Z., Amiinu IS., Cheng R., Wang P., Zhang C., Mu S., Zhao W., Su F., Zhang G., Liao S., Sun S., Single-Atom Catalysts for Electrochemical Hydrogen Evolution Reaction: Recent Advances and Future Perspectives, Nano-*Micro Letters*, 12(1) (2020) 21.

[13] Danilovic N., Subbaraman R., Strmcnik D., Stamenkovic V., Markovic N., Electrocatalysis of the HER in acid and alkaline media, *Journal of the Serbian Chemical Society*, 78(12) (2013) 2007-2015.

[14] Choquette Y., Brossard L., Lasia A., Menard H., Study of the Kinetics of Hydrogen Evolution Reaction on Raney Nickel Composite-Coated Electrode by AC Impedance Technique, *Journal of The Electrochemical Society*, 137(6) (1990) 1723-1730.

[15] Goranova D., Lefterova E., Rashkov R., Electrocatalytic activity of Ni-Mo-Cu and Ni-Co-Cu alloys for hydrogen evolution reaction in alkaline medium, *International Journal of Hydrogen Energy*, 42(48) (2017) 28777-28785.

[16] Farsak M., Kardaş G., Effect of current change on iron-copper-nickel coating on nickel foam for hydrogen production, *International Journal of Hydrogen Energy*, 44(27) (2019) 14151-14156.

[17] Solmaz R., Kardaş G., Fabrication and characterization of NiCoZn–M (M: Ag, Pd and Pt) electrocatalysts as cathode materials for electrochemical hydrogen production, *International Journal of Hydrogen Energy*, 36(19) (2011) 12079-12087.

[18] Farsak M., Aydın Ö., The snowflake-like structured CoO-Cu2O@ Fe/Ru catalyst for hydrogen fuel production, *International Journal of Energy Research*, 45(5) 2020 7561-7571.

[19] Hüner B., Farsak M., Telli E., A new catalyst of AlCu@ZnO for hydrogen evolution reaction, *International Journal of Hydrogen Energy*, 43(15) (2018) 7381-7387.

[20] Mkhondo N., Magadzu T., Surface properties of metal oxides and their role on electrochemical hydrogen storage of carbon nanotubes, *Digest journal of nanomaterials and biostructures*, 13(4) (2018) 921-929.

[21] Rios E., Poillerat G., Koenig JF., Gautier JL., Chartier P., Preparation and characterization of thin Co3O4 and MnCo2O4 films prepared on glass/SnO2:F by spray pyrolysis at 150 °C

for the oxygen electrode, *Thin Solid Films*, 264(1) (1995) 18-24.

[22] Wang K., Xia M., Xiao T., Lei T., Yan W., Metallurgically prepared NiCu alloys as cathode materials for hydrogen evolution reaction, *Mater Chem Phys.*, 186 (2017) 61-66.

[23] Solmaz R., Döner A., Kardaş G., Electrochemical deposition and characterization of NiCu coatings as cathode materials for hydrogen evolution reaction, *Electrochemistry Communications*, 10(12) (2008) 1909-1911.

[24] Telli E., Farsak M., Kardaş G., Investigation of noble metal loading CoWZn electrode for HER, *International Journal of Hydrogen Energy*, 42(36) (2017) 23260-23267.

[25] Tezcan F., Mahmood A., Kardaş G., Optimizing copper oxide layer on zinc oxide via two-step electrodeposition for better photocatalytic performance in photoelectrochemical cells, *Applied Surface Science*, 479 (2019) 1110-1117.

[26] Su D., Kim H-S., Kim W-S., Wang G., Mesoporous Nickel Oxide Nanowires: Hydrothermal Synthesis, Characterisation and Applications for Lithium-Ion Batteries and Supercapacitors with Superior Performance, *Chemistry – A European Journal*, 18(26) (2012) 8224-8229.

[27] Streckova M., Mudra E., Orinakova R., Markusova-Buckova L., Sebek M., Kovalcikova A., Sopcak T., Girman V., Dankova Z., Micusik M., Dusza J., Nickel and nickel phosphide nanoparticles embedded in electrospun carbon fibers as favourable electrocatalysts for hydrogen evolution, *Chem Eng J.*, 303 (2016) 167-181.

[28] Wen T-C., Kang H-M., Co–Ni–Cu ternary spinel oxide-coated electrodes for oxygen evolution in alkaline solution, *Electrochimica Acta*, 43(12) (1998) 1729-1745.

[29] Wang C., Li W., Lu X., Xie S., Xiao F., Liu P., Tong Y., Facile synthesis of porous 3D CoNiCu nano-network structure and their activity towards hydrogen evolution reaction, *International Journal of Hydrogen Energy*, 37(24) (2012) 18688-18693.

[30] Tsoncheva T., Tsyntsarski B., Ivanova R., Spassova I., Kovacheva D., Issa G., Paneva D., Karashanova D., Dimitrov M., Georgieva B., Velinov N., Mitov I., Petrov N., NixZn1-xFe2O4 modified activated carbons from industrial waste as catalysts for hydrogen production, *Microporous and Mesoporous Materials*, 285 (2019) 96-104.

[31] Tasic GS., Maslovara SP., Zugic DL., Maksic AD., Marceta Kaninski MP., Characterization of the Ni–Mo catalyst formed in situ during hydrogen generation from alkaline water electrolysis, *International Journal of Hydrogen Energy*, 36 (18) (2011) 11588-11595.

[32] Stoney GG., The tension of metallic films deposited by electrolysis, *Proceedings of the Royal Society of London Series A, Containing Papers of a Mathematical and Physical Character*, 82(553) (1909) 172-175.

[33] Rosalbino F., Delsante S., Borzone G., Angelini E., Electrocatalytic behaviour of Co–Ni–R (R=Rare earth metal) crystalline alloys as electrode materials for hydrogen evolution reaction in alkaline medium, *International Journal of Hydrogen Energy*, 33(22) (2008) 6696-6703.

[34] Nivetha R., Chella S., Kollu P., Jeong SK., Bhatnagar A., Andrews NG., Cobalt and nickel ferrites based graphene nanocomposites for electrochemical hydrogen evolution, *Journal of Magnetism and Magnetic Materials*, 448 (2018) 165-171.

[35] Hamdani M., Pereira MIS., Douch J., Ait Addi A., Berghoute Y., Mendonça MH., Physicochemical and electrocatalytic properties of Li-Co3O 4 anodes prepared by chemical spray pyrolysis for application in alkaline water electrolysis, *Electrochimica Acta*, 49(9-10) (2004) 1555-1563.

[36] Lačnjevac UČ., Jović BM., Jović VD., Radmilović VR., Krstajić NV., Kinetics of the hydrogen evolution reaction on Ni-(Ebonex-supported Ru) composite coatings in alkaline solution. *International Journal of Hydrogen Energy*, 38(25) (2013) 10178-10190.

[37] Lin H-K., Wang C-B., Chiu H-C., Chien S-H., In situ FTIR Study of Cobalt Oxides for the Oxidation of Carbon Monoxide, *Catalysis Letters*, 86(1) (2003) 63-68.